Authentication of gold nanoparticle encoded pharmaceutical tablets using polarimetric signatures

ARTUR CARNICER,[1,*] ORIOL ARTEAGA,[1,2] JOSEP M. SUÑÉ-NEGRE,[3] AND BAHRAM JAVIDI[4]

[1] *Universitat de Barcelona (UB), Facultat de Física, Departament de Física Aplicada, Martí i Franquès 1, 08028 Barcelona, Catalunya (Spain)*
[2] *FEMAN Group, Institut de Nanociència i Nanotecnologia de la Universitat de Barcelona (IN2UB), 08028 Barcelona, Catalunya (Spain)*
[3] *Universitat de Barcelona (UB), Facultat de Farmàcia, Servei de Desenvolupament del Medicament (SDM), Av. Joan XXIII s/n, 08028 Barcelona, Catalunya (Spain)*
[4] *Electrical and Computer Engineering Department, University of Connecticut, 371 Fairfield Road, Storrs, Connecticut 06269 (USA)*
**Corresponding author: artur.carnicer@ub.edu*

Received XX Month XXXX; revised XX Month, XXXX; accepted XX Month XXXX; posted XX Month XXXX (Doc. ID XXXXX); published XX Month XXXX

Counterfeiting of pharmaceutical products represents concerns for both the industry and general public safety. Falsification produces losses to companies and poses health risks for patients. In order to detect fake pharmaceutical tablets, we propose producing film-coated tablets with gold nanoparticle encoding. These coated tablets contain unique polarimetric signatures. We present experiments to show that ellipsometric optical techniques in combination with machine learning algorithms can be used to distinguish among genuine and fake samples. To the best of our knowledge this is the first report on using gold nanoparticles encoding with optical polarimetric classification for anti-counterfeiting of pharmaceutical products. © 2016 Optical Society of America

***OCIS codes**: (100.4998) Pattern recognition, optical security and encryption, (260.5430) Polarization, (240.0310) Ellipsometry and polarimetry, (150.0150) Machine vision.*

http://dx.doi.org/10.1364/OL.99.099999

Optical techniques have been suggested for authentication and anti counterfeiting [1] mainly by using optically encoded tags. In recent years, the use of metal nanoparticles has been present in multiple fields of science and technology. In particular, gold nanoparticles (AuNP) are widely used in biology and medicine since they are considered non-toxic and biocompatible [2-4]. Multiple applications for AuNP in biomedicine have been described. Among many others, AuNP are being used as labeling, delivery, heating, or gene-regulating agents. They also play a role in photo-responsive therapeutics or as drug carriers [5-6] and, due to their particular scattering properties, AuNP can be used in imaging diagnostic systems [7-8]. AuNP display interesting scattering and polarization properties that depend on the size and form of the nanoparticles [9-11]. Nanoparticle structures can be used for security and counterfeit applications. Subtle changes in the polarimetric signature can be detected and subsequently processed using machine learning algorithms. These pattern recognitions techniques are able to distinguish among true and false classes with high confidence [12-13]. Counterfeiting of pharmaceutical products represents a major concern for both the industry and the general public [14-18]. These kinds of counterfeiting activities produces losses to companies and can result in severe health risks for those who take fake medicines obtained outside the regulated distribution system. In order to detect possible counterfeiting in pharmaceutical tablets (a.k.a. pills), we propose producing film-coated tablets with AuNP. Such film-coated tablets will become polarimetrically labeled and can produce a unique polarimetric signal that enables distinguishing among authentic and false classes of tablets. To the best of our knowledge this is the first report on using AuNP in pharmaceutical products for anti-counterfeiting using polarimetric techniques and machine learning classification algorithms.

This paper is organized as follows: first we describe the fabrication process for obtaining AuNP film-coated tablets. Then, we review basic polarimetric principles used in the analysis of the tablets. Experimental device is also described. Experimental results and analysis of data are presented and discussed.

Flat tablets with a diameter of 10 mm, coated with hydroxypropyl methylcellulose (HPMC) were prepared according to the formulation presented in Table 1. HMPC is a safe and inert product, widely used as excipient in pharmaceutical coatings [19]. AuNP were obtained from three commercial solutions (Endor Nanotechnologies) with different concentrations: 0.05 mg/ml for the 4 nm AuNP, 0.03 mg/ml for the 12 nm samples and 0.01 mg/ml for the 25 nm nanoparticles. In all cases, dispersity index Đ (a measure of heterogeneity of sizes of particles) was close to 1.

Table 1: tablets and coating components

Tablet components:	Lactose monohydrate (Tablettose® 80)	35%
	Microcrystalline cellulose (Vivapur® 101)	59%
	Talc	4%
	Magnesium stearate	2%
Tablet coating:	Hydroxypropyl methylcellulose (HPMC) (Pharmacoat® 606)	3%
	Deionized water	97%

The components of the tablets were weighed and screened through a 0.8 mm mesh sieve and subsequently mixed during 30 minutes in a biconic mixer at a speed of 20 rpm. Then, direct compression of the mixture using an eccentric tableting machine was carried out. This instrument was adjusted to produce tablets with a weight of 270 mg and a hardness of about 100 N. The 4, 12 and 25 nm AuNP were dispersed in different containers by means of mechanical agitation. A fourth group of film-coated tablets was produced without nanoparticles. We will refer to them as placebo film-coated tablets. The solutions were filtered through a sieve 0.212 mm wide.

The film-coated tablets obtained are indistinguishable under visual inspection or using conventional image processing techniques. Figure 1(a) shows 8 film-coated tablets of the four classes as they were mounted in sample holder of the instrument. An extra pill, that was not measured, also appears on the image as it was used for the initial alignment of the sample holder. A schematic of the instrument is shown in Fig. 1(b). Note that tablets are isotropic so their orientation does not matter

.

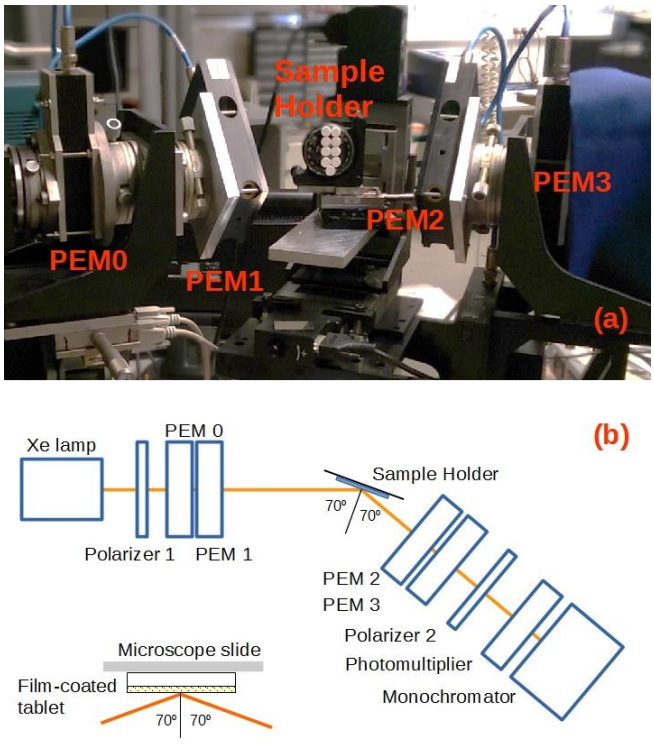

Fig. 1. (a) Experimental set up. Film-coated tablets as they were mounted in sample holder of the instrument. PEMs are the photoelastic modulators. (b) Schematic of the Mueller matrix ellipsometer device setup.

The Mueller matrix used in the analysis is noted as:

$$\mathbf{M} = \begin{pmatrix} m_{00} & m_{01} & m_{02} & m_{03} \\ m_{10} & m_{11} & m_{12} & m_{13} \\ m_{20} & m_{21} & m_{22} & m_{23} \\ m_{30} & m_{31} & m_{32} & m_{33} \end{pmatrix} \quad \textbf{(1)}$$

It provides a complete polarimetric description of the sample. The polarization state of the beam after interacting with a tablet is **S'=MS**, where $\mathbf{S} = (S_0, S_1, S_2, S_3)$ and $\mathbf{S}' = (S'_0, S'_1, S'_2, S'_3)$ are the Stokes vectors of the incident and the reflected light respectively. If the sample is isotropic the normalized Mueller $\mathbf{M_0}$ is highly symmetric and some of its components are zero:

$$\mathbf{M_0} = \begin{pmatrix} 1 & -N & 0 & 0 \\ -N & 1 & 0 & 0 \\ 0 & 0 & C & S \\ 0 & 0 & -S & C \end{pmatrix} \quad \textbf{(2)}$$

with $N = \cos(2\psi)$, $C = \sin(2\psi)\cos\Delta$, and $S = \sin(2\psi)\sin\Delta$.

Ellipsometric angles ψ and Δ are related to the complex Fresnel reflection coefficients for p- and s- polarized light (r_{pp} and r_{ss}, respectively) by means of $\frac{r_{pp}}{r_{ss}} = \tan\psi \exp(i\Delta)$. For more insight about ellipsometric techniques and the Mueller matrix see, for instance, references [20, 21].

The Mueller matrix ellipsometer used for measurements was described in [22-23]. This instrument uses four photoelastic modulators (PEMs) with different frequencies to modulate the polarization state of light both before and after the sample [Fig. 1(b)]. Fourier analysis of the time varying signal delivers simultaneously all sixteen elements of the Mueller matrix with high precision. All ellipsometric measurements were done with an angle of incidence of 70º, using a spot size of approximately 8 mm x 6 mm that impinged at the center of each tablet. The film-coated tablets were glued on a microscope slide and then mounted in the sample holder of the instrument. The selection of the target pill that is measured was done by moving the vertical or lateral translators of the sample holder.

Our film-coated tablets can be roughly considered as a turbid medium in which light can be scattered consecutively several times before leaving the medium, thus introducing some depolarization. It is expected that metallic nanoparticles of different sizes will distinctively modify this depolarizing behavior [10-12]. This fact is used to discriminate among the different classes of film-coated tablets. We measured the Mueller matrix components for two film-coated tablets representative of each class, using the instrument described above. The measurements were spectroscopic beam in the range 280 to 700 nm. Results are presented in Fig. 2, where black, red, green and blue curves stand for placebo, 4, 12, and 25 nm film-coated tablets. Two film-coated tablets of each class have been measured.

Despite the fact that Mueller matrix components can take values between -1 and 1, for the sake of readability the y-scale of the plots matches their respective dynamic ranges. Note that components $m_{01} = m_{10}$, m_{22}, $m_{23} = -m_{23}$ *and* m_{33} provide distinctive information; m_{00} is, because of the normalization, equal to one and component

m_{11} is nearly 1 within the considered range. The rest of the components are very close to zero and fluctuations can be considered measurement noise. Generally speaking, samples behave in a very close manner to isotropic materials since they approximately follow the polarimetric Mueller matrix model described in Eq. (2).

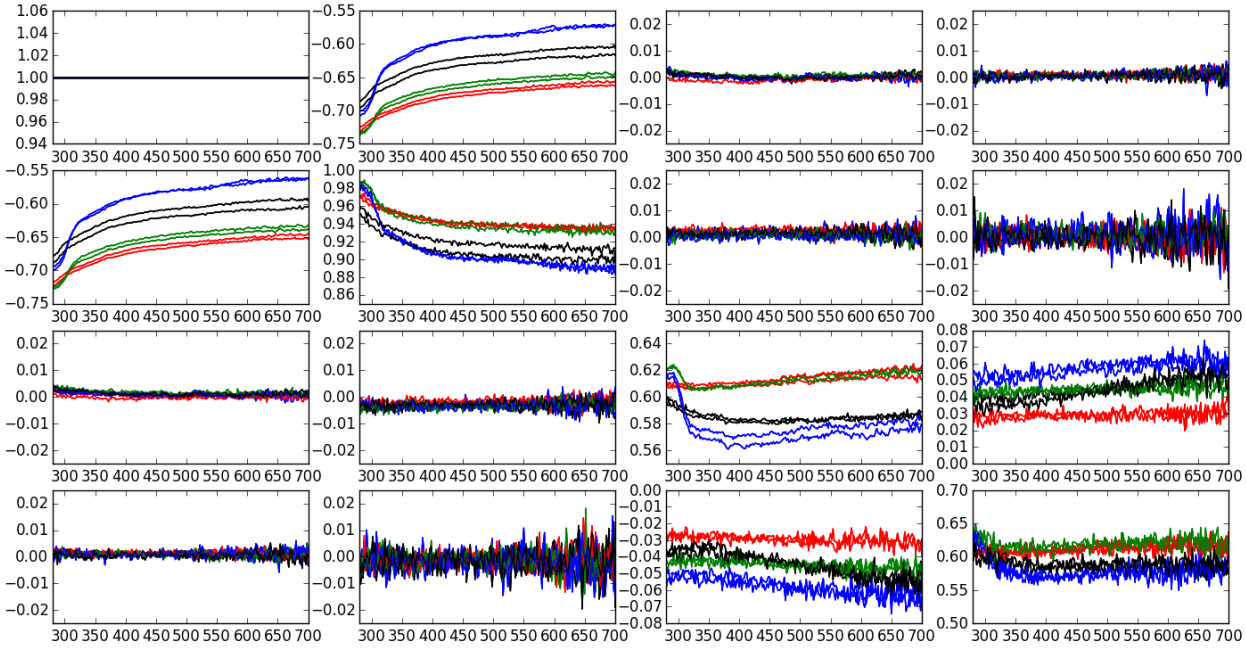

Fig. 2. Mueller matrix elements [see Eq. (1)] as a function of the wavelength for nanogold particle encoded tablets. The y-scale of the plots matches the respective dynamic ranges of the components. Two tablets of each set were measured. Black: placebo film-coated tablets; red: film-coated tablets with 4 nm AuNP; green: film-coated tablets with 12 nm AuNP; blue: film-coated tablets with 25 nm AuNP.

The degree of polarization DoP is an effective way to describe the behavior of the samples with a single parameter. The DoP of a beam described by the Stokes vector **S** is defined as

$$\mathrm{DoP} = \frac{\sqrt{S_1^2 + S_2^2 + S_3^2}}{S_0}. \qquad \textbf{(3)}$$

We calculate the DoP as a function of the wavelength for several polarization states of the input beam represented by the following Stokes vectors: (1,0,0,0), (1,1,00), (1,-1,0,0), (1,0,1,0), (1,0,-1,0), (1,0,0,1) and (1,0,0,-1). The eight tablets considered are taken into account. Results are presented in Fig. 3. In general, the DoP is nearly constant within the range 350-700 nm. Note that for the cases S=(1,0,0,1) (clockwise circularly polarized light) or S=(1,1,0,0) (x-direction linearly polarized light) results are noisier. Then, the DoP as a function of the wavelength for all possible states of the Stokes vector $\mathbf{S} = (1, \cos 2\psi, \sin 2\psi, 0)$ is calculated, where the polarization angle ψ ranges from 0 to 90º. The averaged value of the DoP (for wavelengths within the range 350 to 700 nm) is shown in Fig. 4. Note that the errors bars indicate the standard deviation of the DoP for the corresponding angle ψ. It is apparent that that for angles $\psi \in [20º, 35º]$, the DoP of the two samples that belong to the same class display very similar values, i.e. both curves nearly overlap. Moreover, the behavior of the DOP for the placebo and the 4 nm AuNP film-coated tablets is very similar and can hardly be distinguished for ψ>40º.

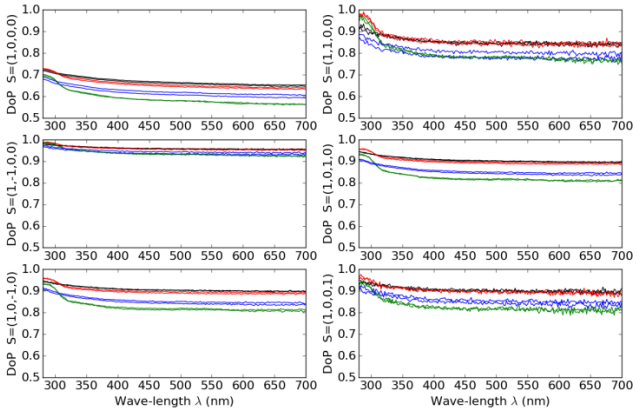

Fig. 3. DoP as a function of the wavelength for different polarization states: Black curves: placebo film-coated tablets; red curves: film-coated tablets with 4 nm AuNP; green curves: film-coated tablets with 12 nm AuNP; Blue curves: film-coated tablets with 25 nm AuNP.

A possible way to circumvent errors in film-coated tablets classification is by using machine learning algorithms. For classification purposes we take the k-nearest neighbors (kNN) algorithm [24]. This is a very powerful unsupervised classification

method but relatively easy to implement. kNN tries to determine the class the current sample belongs to by considering the majority of the k closest samples of the training set. The scikit-learn library is used to perform calculations [25]. Classification methods require sufficient data to train the system: we evaluate the DoP as a function of the wavelength (in the range 350 to 700 nm), when the sample is illuminated with linearly polarized light; the polarization angle ψ ranges from 20º to 35º with a step size of 0.057º (0.001 rad). We use a hold-out strategy to divide the dataset into training and test sets: the training set was generated by selecting randomly half of the samples of the four classes. The mean accuracy (total number of samples correctly classified divided by the total number of test samples) is used to evaluate classification capability [26]. The algorithm was run 1000 times using different combinations of samples as the training set. We set k=1. The classification accuracy was equal 1, so successful classification of the film-coated tablets is possible using the DoP estimated from the Mueller matrix analysis.

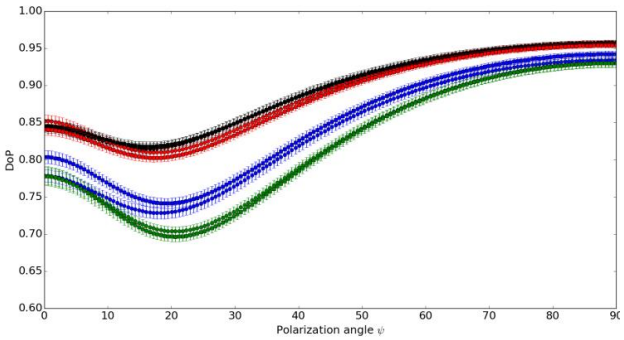

Fig. 4. Averaged DoP as a function of the polarization angle. Error bars show the standard deviation. The mean is calculated in the range 350-700 nm. Black dots: placebo film-coated tablets; red dots: film-coated tablets with 4 nm AuNP; Green dots: film-coated tablets with 12 nm AuNP; blue dots: film-coated tablets with 25 nm AuNP.

A second test using kNN algorithm was conducted. In this case, the DoP data set generated by four film-coated tablets, each one representing its corresponding class, is used to train the system whereas the data provided by the other film-coated tablets is used to test the classification. We took into account the 16 possible combinations. In all cases considered the classification accuracy was equal to 1. In conclusion, the system can be trained with the data obtained from a set of AuNP film-coated tablets.

In summary, we propose using polarimetric authentication and verification of nano particle encoded pharmaceutical tablets. Experiments are presented by producing film-coated with AuNP as a way to detect possible counterfeiting in pharmaceutical tablets. Film-coated tablets become polarimetrically labeled and thus they can be distinguished among authentic and counterfeit classes of tablets. During the fabrication process, AuNP of 4, 12 and 25 nm of size were dispersed on the coating of three different sets of otherwise identical film-coated tablets. We also produced a fourth group of film-coated tablets that do not contain AuNP. The analysis of the samples was performed using a Mueller matrix ellipsometer able to produce information in the range 280 to 700 nm. The information provided by this device is used to calculate the DoP. By means of the kNN classification algorithm we demonstrate that successful authentication is possible and that the film-coated tablets can be unambiguously distinguished without error. The present results show successful classification using four classes of tablets. More complex and realistic scenarios with a variety of tablets coated with multiple AuNP sizes can be considered as well using more powerful classification techniques trained with a larger number of samples. Other polarimetric and/or recognition approaches may be used [27].

Funding. A. Carnicer acknowledges support from Ministerio de Economía y Competitividad (Spain) project FIS2013-46475-C3-2-P. B. Javidi acknowledges support under NSF ECCS 1545687.

Acknowledgment. We are indebted to Dr. Maria Canals and Dr. Robert Saborit for fruitful discussions and suggestions. Endor Nanotechnologies provided free gold nanoparticles samples.

REFERENCES

1. O. Matoba, T. Nomura, E. Perez-Cabre, M. S. Millan, and B. Javidi, Proc. of IEEE **97**, 1128-1148 (2009).
2. R. Shukla, V. Bansal, M. Chaudhary, A. Basu, R. R. Bhonde, M. Sastry, Langmuir **21**, 10644-10654 (2005).
3. P. Ghosh, G. Han, M. De, C- K. Kim, and V. M. Rotello, Adv. Drug. Deliv. Rev. **60**, 1307-1315 (2008).
4. E. Boisselier, and D. Astruc, Chem. Soc. Rev **38**, 1759-1782 (2009).
5. R. A. Sperling, P. Rivera Gil, F. Zhang, M. Zanella, and W. J. Parak, Chem. Soc. Rev **37**, 1896-1908 (2008).
6. D. A. Giljohann, D. S. Seferos, W. L. Daniel, M. D. Massich, P. C. Patel, and C. A. Mirkin, Angew. Chem. Int. Ed. **49**, 3280-3294 (2010).
7. A. J. Mieszawska, W. J. Mulder, Z. A. Fayad, and D. P. Cormode, Mol. Pharm. **10**, 831-847 (2013).
8. P. K. Jain, K. S. Lee, I. H. El-Sayed, M. A. El-Sayed, J. Phys. Chem. B **110**, 7238– 7248 (2006).
9. T. Ming, L. Zhao, Z. Yang, H. Chen, L. Sun, J. Wang, C. Yan, Nano Lett. **9** 3896-3903 (2009].
10. J. Aaron, E. de la Rosa, K. Travis, N. Harrison, J. Burt, M. José-Yacamán, and K. Sokolov, Opt. Express **16**, 2153-2167 (2008).
11. U. Guler, R. Turan, Opt. Express **18**, 17322-17338 (2010).
12. A. Carnicer, A. Hassanfiroozi, P. Latorre-Carmona, Y.-P. Huang, and B. Javidi, Opt. Lett. **40**, 135-138 (2015).
13. A. Carnicer, O. Arteaga, E. Pascual, A. Canillas, S. Vallmitjana, B. Javidi, and E. Bertran, Opt. Lett. **40**, 5399-5402 (2015)
14. E. Medina, E. Bel, J.M. Suñé, British Medical Journal Open. **4**, 6: e010387 (2016).
15. K. Dégardin, Y. Roggo, P. Margot, J. Pharm Biomed. Anal. **87**, 167-175 (2014).
16. Bull. World Health. Organ. **88** 247–248 (2010).
17. S. Kovacs, S. E. Hawes, S. N. Maley, PLoS One **26**, e90601 (2014).
18. D. Bansal, S. Malla, K. Gudala, P. Tiwari, Sci Pharm. **81**, 1-13 (2013).
19. R. C. Rowe, P. J. Sheskey, and P. J. Weller, eds. Handbook of pharmaceutical excipients. (Pharmaceutical Press, 2012.)
20. E. Collett, Field Guide to Polarization, (SPIE Press, 2005).
21. O. Arteaga, Thin Solid Films **571**, 584–588 (2014).
22. O. Arteaga, J. Freudenthal, B. Wang, and B. Kahr, " Appl. Opt. 51, 6805-6817 (2012)
23. O. Arteaga, M. Baldrís, J. Antó, A. Canillas, E. Pascual, and E. Bertran, Appl. Opt. **53**, 2236-2245 (2014).
24. T. M. Cover and P. E. Hart, IEEE Trans. Inf. Theory **13**, 21-27 (1967).
25. F. Pedregosa, G. Varoquaux, A. Gramfort, V. Michel, B. Thirion, O. Grisel, M. Blondel, P. Prettenhofer, R. Weiss, V. Dubourg, J. Vanderplas, A. Passos, D. Cournapeau, M. Brucher, M. Perrot, and E. Duchesnay, J. Mach. Learn. Res. **12**, 2825- 2830 (2011).
26. N. Japkowicz and M. Shah, Evaluating Learning Algorithms: a Classification Perspective (Cambridge University, 2011).
27. F. A. Sadjadi, A. Mahalanobis, Appl. Opt. 45, 3063-3070 (2006).

FULL REFERENCES

1. O. Matoba, T. Nomura, E. Perez-Cabre, M. S. Millan, and B. Javidi, "Optical Techniques for Information Security," Proc. of IEEE 97, 1128-1148 (2009).
2. R. Shukla, V. Bansal, M. Chaudhary, A. Basu, R. R. Bhonde, M. Sastry, "Biocompatibility of gold nanoparticles and their endocytotic fate inside the cellular compartment: a microscopic overview," Langmuir **21**, 10644-10654 (2005).
3. P. Ghosh, G. Han, M. De, C- K. Kim, and V. M. Rotello, "Gold nanoparticles in delivery applications," Adv. Drug. Deliv. Rev. **60**, 1307-1315 (2008).
4. E. Boisselier, and D. Astruc, "Gold nanoparticles in nanomedicine: preparations, imaging, diagnostics, therapies and toxicity," Chem. Soc. Rev **38**, 1759-1782 (2009).
5. R. A. Sperling, P. Rivera Gil, F. Zhang, M. Zanella, and W. J. Parak, "Biological applications of gold nanoparticles," Chem. Soc. Rev **37**, 1896-1908 (2008).
6. D. A. Giljohann, D. S. Seferos, W. L. Daniel, M. D. Massich, P. C. Patel, and C. A. Mirkin, "Gold nanoparticles for biology and medicine," Angew. Chem. Int. Ed. **49**, 3280-3294 (2010).
7. A. J. Mieszawska, W. J. Mulder, Z. A. Fayad, and D. P. Cormode, "Multifunctional gold nanoparticles for diagnosis and therapy of disease," Mol. Pharm. **10**, 831-847 (2013).
8. P. K. Jain, K. S. Lee, I. H. El-Sayed, M. A. El-Sayed, "Calculated absorption and scattering properties of gold nanoparticles of different size, shape, and composition: applications in biological imaging and biomedicine," J. Phys. Chem. B **110**, 7238– 7248 (2006).
9. T. Ming, L. Zhao, Z. Yang, H. Chen, L. Sun, J. Wang, C. Yan, "Strong polarization dependence of plasmon-enhanced fluorescence on single gold nanorods," Nano Lett. **9** 3896-3903 (2009].
10. J. Aaron, E. de la Rosa, K. Travis, N. Harrison, J. Burt, M. José-Yacamán, and K. Sokolov, "Polarization microscopy with stellated gold nanoparticles for robust, in-situ monitoring of biomolecules," Opt. Express **16**, 2153-2167 (2008).
11. U. Guler, R. Turan, "Effect of particle properties and light polarization on the plasmonic resonances in metallic nanoparticles," Opt. Express **18**, 17322-17338 (2010).
12. A. Carnicer, A. Hassanfiroozi, P. Latorre-Carmona, Y.-P. Huang, and B. Javidi, "Security authentication using phase-encoded nanoparticle structures and polarized light," Opt. Lett. **40**, 135-138 (2015).
13. A. Carnicer, O. Arteaga, E. Pascual, A. Canillas, S. Vallmitjana, B. Javidi, and E. Bertran, "Optical security verification by synthesizing thin films with unique polarimetric signatures," Opt. Lett. **40**, 5399-5402 (2015).
14. E. Medina, E. Bel, JM Suñé, "Counterfeit medicines in Peru: a retorspective review (1997-2014)". British Medical Journal Open. **4**, 6: e010387 (2016).
15. K. Dégardin, Y. Roggo, P. Margot, "Understanding and fighting the medicine counterfeit market," J. Pharm Biomed. Anal. **87**, 167-175 (2014).
16. World Health Organization. "Growing threat from counterfeit medicines," Bull. World Health. Organ. **88** 247–248 (2010).
17. S. Kovacs, S. E. Hawes, S. N. Maley, "Technologies for detecting falsified and substandard drugs in low and middle-income countries," PLoS One **26**, e90601 (2014).
18. D. Bansal, S. Malla, K. Gudala, P. Tiwari, "Anti-counterfeit technologies: a pharmaceutical industry perspective," Sci Pharm. **81**, 1-13 (2013).
19. R. C. Rowe, P. J. Sheskey, and P. J. Weller, eds. Handbook of pharmaceutical excipients. Pharmaceutical Press, London (2006.)
20. E. Collett, Field Guide to Polarization, SPIE Press, Bellingham, WA (2005).
21. O. Arteaga, "Useful Mueller matrix symmetries for ellipsometry," Thin Solid Films **571**, 584–588 (2014).
22. O. Arteaga, J. Freudenthal, B. Wang, and B. Kahr, "Mueller matrix polarimetry with four photoelastic modulators: theory and calibration," Appl. Opt. 51, 6805-6817 (2012)
23. O. Arteaga, M. Baldrís, J. Antó, A. Canillas, E. Pascual, and E. Bertran, "Mueller matrix microscope with a dual continuous rotating compensator setup and digital demodulation," Appl. Opt. **53**, 2236-2245 (2014).
24. T. M. Cover and P. E. Hart, "Nearest neighbor pattern classification," IEEE Trans. Inf. Theory **13**, 21-27 (1967).
25. F. Pedregosa, G. Varoquaux, A. Gramfort, V. Michel, B. Thirion, O. Grisel, M. Blondel, P. Prettenhofer, R. Weiss, V. Dubourg, J. Vanderplas, A. Passos, D. Cournapeau, M. Brucher, M. Perrot, and E. Duchesnay, "Scikit-learn: Machine learning in Python," J. Mach. Learn. Res. **12**, 2825- 2830 (2011).
26. N. Japkowicz and M. Shah, Evaluating Learning Algorithms: a Classification Perspective (Cambridge University, 2011).
27. F. A. Sadjadi and A. Mahalanobis, "Target-adaptive polarimetric synthetic aperture radar target discrimination using maximum average correlation height filters," Appl. Opt. **45**, 3063-3070 (2006)